Rapid Inversion at Phosphorus in the $[\eta^4\text{-}(C_6H_{11})_3SnP_7W(CO)_3]^{2-}$ and $[(en)(CO)_3W(\eta^1,\eta^4\text{-}P_7)M(CO)_3]^{3-}$ Ions Where M = Cr, W

Scott Charles, Janet A. Danis, James C. Fettinger, and Bryan W. Eichhorn*

Department of Chemistry and Biochemistry, University of Maryland, College Park, Maryland 20742

Received September 25, 1996[⊗]

Ethylenediamine (en) solutions of $[\eta^4\text{-}P_7M(CO)_3]^{3-}$ ions [M = Cr (**1a**), W (**1b**)] react with (mesitylene)$W(CO)_3$ to form the bimetallic complexes $[(en)(CO)_3W(\eta^1,\eta^4\text{-}P_7)M(CO)_3]^{3-}$ where M = Cr (**3a**), W (**3b**) in good yield. Compound **3b** can be prepared directly from P_7^{3-} and 2 equiv of (mesitylene)$W(CO)_3$. Compound **3a** reacts with 1 equiv of P_7^{3-} to form **1a** and **1b**. En solutions of **1b** react with 1 equiv of $(C_6H_{11})_3SnCl$ to give $[\eta^4\text{-}(C_6H_{11})_3SnP_7W(CO)_3]^{2-}$ (**4**) in good crystalline yield as the $[K(2,2,2\text{-crypt})]^+$ salt. The X-ray structure of the $[K(2,2,2\text{-crypt})]^+$ salt **3b** revealed a norbornadiene-like P_7 cage bound η^4 to the $W(CO)_3$ fragment (*cf.* $[\eta^4\text{-}P_7W(CO)_3]^{3-}$) and η^1 to the (en)$(CO)_3$W fragment via the long W(2)−P(1) bond of 2.643(3) Å. The structure of **4** is similar, with a $(C_6H_{11})_3Sn^+$ group attached to the P(1) atom of the $[\eta^4\text{-}P_7W(CO)_3]^{3-}$ complex. The coordination geometry at P(1) is distinctly pyramidal in both compounds, which leaves the ions with no crystallographic symmetry. For complexes **3a** and **3b**, two fluxional processes are rapid on the NMR time scale at −50 °C (202 MHz) that give the P_7 cages virtual C_{2v} symmetry in solution and AA′A″A‴MM″X spin systems. These processes are (1) a wagging of the four P atoms bound to the $M(CO)_3$ units and (2) rapid inversion at P(1). For **4**, inversion at phosphorus becomes slow on the NMR time scale at low temperature (−50 °C, 83 MHz) with $\Delta G^{\ddagger} = 13$ kcal/mol. Crystallographic data are as follows. $[K(2,2,2\text{-crypt})]_3$**3b**·en: triclinic, $P\bar{1}$, $a = 14.396(4)$ Å, $b = 17.543(3)$ Å, $c = 20.518(2)$ Å, $\alpha = 82.419(11)°$, $\beta = 76.830(14)°$, $\gamma = 69.16(2)°$, $V = 4708(2)$ Å^3, $Z = 2$, $R(F) = 5.52\%$, $R_w(F^2) = 14.31\%$. $[K(2,2,2\text{-crypt})]_2$**4**: triclinic, $P\bar{1}$, $a = 12.247(2)$ Å, $b = 15.1909(14)$ Å, $c = 21.292(3)$ Å, $\alpha = 97.374(10)°$, $\beta = 93.273(13)°$, $\gamma = 111.217(9)°$, $V = 3639.8(8)$ Å^3, $Z = 2$, $R(F) = 10.50\%$, $R_w(F^2) = 20.21\%$.

Introduction

The chemistry of the $[\eta^4\text{-}P_7M(CO)_3]^{3-}$ ions (**1**) where M = Cr, Mo, W[1−3] is characterized by markedly different reactions with electrophiles and nucleophiles. Electrophiles attack at the phosphorus atom furthest from the transition metal (the P(1) site)[2,4,5] whereas the nucleophile CO reacts at the transition metal center.[6] The electrophilic reactivity can be understood by examining the electronic structures of **1**, which show high-lying

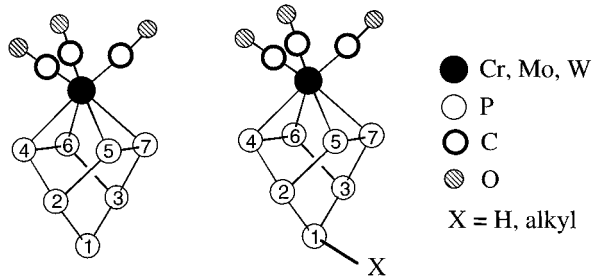

1 **2**

ligand-based lone pairs localized on the P(1) atoms.[2] As a consequence, various electrophiles (*i.e.*, H^+, CH_3^+) attack **1** at the P(1) site to form generic $[\eta^4\text{-}XP_7M(CO)_3]^{2-}$ complexes (**2**) where X = H^+,[2,5] R^+.[4] The solid state and solution structures of these compounds show distinctly pyramidal geometry at P(1), as expected from valence bond considerations (see drawing of **2**). The pyramidal geometry at P(1) renders the P(4), P(6) and P(5), P(7) pairs of atoms *inequivalent*, in contrast to the symmetrical structure of **1**, where all four atoms are chemically equivalent on the NMR time scale.

In related chemistry, the parent P_7^{3-} ion can be alkylated to form mixtures of the symmetric (minor) and unsymmetric (major) isomers of the neutral $R_2R'P_7$ molecules where R = Me, Et, *n*-Bu, CH_2Ph.[4] Formation of the symmetric minor isomers requires inversion of configuration at one P atom during the alkylation process, but the two isomers do not interconvert in solution once they are formed (*i.e.*, no phosphorus inversion). Baudler and co-workers[7−9] have thoroughly studied the spectroscopic properties and solution dynamics of related polycyclic phosphanes which occasionally show phosphorus inversion barriers (E_a) as low as 18.5 kcal/mol. Facile inversion at phosphorus is usually associated with those atoms bound to "bulky, electropositive substituents". The origins of the low inversion barriers in these compounds have been attributed to combinations of steric and electronic factors although the specific roles of these factors are not well understood. Our long-term goals are to identify which compounds show rapid phosphorus inversion and to study these processes in a systematic way. We report here the synthesis and characterization of two new types of compounds that show rapid inversion at phosphorus on the NMR time scale, namely $[(en)(CO)_3W(\eta^1,\eta^4\text{-}P_7)M(CO)_3]^{3-}$ (**3**) where M = Cr, W and $[\eta^4\text{-}(C_6H_{11})_3$-

[⊗] Abstract published in *Advance ACS Abstracts,* June 1, 1997.

(1) Eichhorn, B. W.; Haushalter, R. C.; Huffman, J. C. *Angew. Chem., Int., Ed. Engl.* **1989**, *28*, 1032.
(2) Charles, S.; Bott, S. G.; Rheingold, A. L.; Eichhorn, B. W. *J. Am. Chem. Soc.* **1994**, *116*, 8077.
(3) Bolle, U.; Tremel, W. *J. Chem. Soc., Chem. Commun.* **1994**, 217.
(4) Charles, S.; Fettinger, J. C.; Eichhorn, B. W. *J. Am. Chem. Soc.* **1995**, *117*, 5303.
(5) Charles, S.; Fettinger, J. C.; Eichhorn, B. W. Results to be published.
(6) Charles, S.; Eichhorn, B. W.; Fettinger, J. C.; Bott, S. G. *Inorg. Chem.* **1996**, *35*, 1540.
(7) Baudler, M. *Angew. Chem., Int. Ed. Engl.* **1987**, *26*, 419.
(8) Baudler, M.; Glinka, K. *Chem. Rev.* **1993**, *93*, 1623.
(9) Baudler, M.; Deriesemeyer, L. *Z. Naturforsch.* **1996**, *B51*, 101.

S0020-1669(96)01177-9 CCC: $14.00

$SnP_7W(CO)_3]^{2-}$ (**4**). The former compounds represent rare examples of mixed-metal Zintl ion complexes.[10]

Results

Syntheses. Ethylenediamine (en) solutions of [K(2,2,2-crypt)]$_3$[η^4-$P_7M(CO)_3$] where M = Cr, W react with 1 equiv of (mesitylene)$W(CO)_3$ to form [(en)$(CO)_3W(\eta^1,\eta^4$-$P_7)M(CO)_3]^{3-}$ ions (**3**) according to eq 1. The reactions give high conversions

$$[\eta^4\text{-}P_7M(CO)_3]^{3-} + (\text{mesitylene})W(CO)_3 \xrightarrow{\text{en}} [(\text{en})(CO)_3W(\eta^1,\eta^4\text{-}P_7)M(CO)_3]^{3-} + \text{mesitylene} \quad (1)$$
$$M = Cr\ (\mathbf{3a}),\ W\ (\mathbf{3b})$$

(^{31}P NMR analysis) and proceed at modest rates at ambient temperatures ($t_{1/2} \approx 1$ h). Compounds **3** have been isolated in good crystalline yields as [K(2,2,2-crypt)]$^+$ salts (**3a**, 53%; **3b**, 60%). The salts are orange and air and moisture sensitive and have been characterized by IR and ^{1}H, ^{13}C, and ^{31}P NMR spectroscopic studies as well as elemental analyses and, for **3b**, single-crystal X-ray diffraction. They can also be prepared in DMF solutions (quantitative conversion according to ^{31}P NMR analysis) to presumably give $[(DMF)_2(CO)_3W(\eta^1,\eta^4$-$P_7)M(CO)_3]^{3-}$ complexes; however, these compounds have not been isolated. Compound **3b** can be prepared directly from P_7^{3-} and 2 equiv of (mesitylene)$W(CO)_3$ in en without 2,2,2-crypt (eq 2) whereas

$$P_7^{3-} + 2(\text{mesitylene})W(CO)_3 \xrightarrow{\text{en}} [(\text{en})(CO)_3W(\eta^1,\eta^4\text{-}P_7)W(CO)_3]^{3-} + 2\ \text{mesitylene} \quad (2)$$
$$\mathbf{3b}$$

the formation **3a** requires the use of the [K(2,2,2-crypt)]$_3$[η^4-$P_7Cr(CO)_3$] precursor, as shown in eq 1. As in the case of the protonated and alkylated derivatives, **2**,[4,5] the $L_2(CO)_3W$ groups (L_2 = en or 2 DMF) of **3** are attached to the [η^4-$P_7M(CO)_3]^{3-}$ clusters at the P(1) site.

Compound **3a** reacts with 1 equiv of K_3P_7 to give **1a** and **1b** according to eq 3.

$$[(\text{en})(CO)_3W(\eta^1,\eta^4\text{-}P_7)Cr(CO)_3]^{3-} + P_7^{3-} \xrightarrow{\text{en}} [\eta^4\text{-}P_7Cr(CO)_3]^{3-} + [\eta^4\text{-}P_7W(CO)_3]^{3-} \quad (3)$$
$$\mathbf{3a} \qquad\qquad \mathbf{1a} \qquad\qquad \mathbf{1b}$$

Ethylenediamine solutions of **1b** react with 1 equiv of $(C_6H_{11})_3SnCl$ to give the [η^4-$(C_6H_{11})_3SnP_7W(CO)_3]^{2-}$ ion (**4**) after 8 h at room temperature according to eq 4. Dark red

$$[\eta^4\text{-}P_7W(CO)_3]^{3-} + (C_6H_{11})_3SnCl \xrightarrow{\text{en}} [\eta^4\text{-}(C_6H_{11})_3SnP_7W(CO)_3]^{2-} + Cl^- \quad (4)$$
$$\mathbf{1b} \qquad\qquad \mathbf{4}$$

crystals of the [K(2,2,2-crypt)]$^+$ salt of **4** were precipitated from warmed (~40 °C) en solutions in 42% isolated yield. The compound is air sensitive in solution and in the solid state and has been characterized by IR, ^{1}H NMR, ^{13}C NMR, and variable-temperature ^{31}P NMR spectroscopic studies as well as single-crystal X-ray diffraction and elemental analysis.

Structural Studies. The [K(2,2,2-crypt)]$^+$ salt of **3b** is triclinic, space group $P\bar{1}$, and crystallizes with two en solvate molecules. An ORTEP drawing of the [(en)$(CO)_3W(\eta^1,\eta^4$-$P_7)W(CO)_3]^{3-}$ anion is shown in Figure 1. A summary of the crystallographic data is given in Table 1, and a listing of selected bond distances and angles is given in Table 2. The structure contains a norbornadiene-like P_7^{3-} cluster that is bound η^4 to the $W(CO)_3$ fragment and η^1 to the $W(CO)_3$(en) fragment. The central η^4-$P_7W(CO)_3$ unit is very similar to the structurally characterized [η^4-$P_7Cr(CO)_3]^{3-}$ anion[2] and related compounds.[4] The W(1)−P bond distances to the four tungsten-bound phosphorus atoms average 2.64(5) Å and are similar to those observed for [η^4-$(CH_3CH_2)P_7W(CO)_3]^{2-}$, **5**.[4] The P(4)- and P(5)-to-W(1) distances are 2.596(8) Å (average) whereas the P(6) and P(7) contacts to W(1) are slightly longer at 2.672(6) Å (average) due to the *trans* orientation of these atoms with respect to the carbonyl carbons C(3) and C(2), respectively (P−W−C = 173(1)°, average). As a result, the P(4)···P(5) and P(6)···P(7) separations are asymmetric at 2.873(5) and 3.192(5) Å, respectively, which is again typical for these types of compounds.[2−4,11,12] The remaining P−P bond distances range from 2.135(5) to 2.232(5) Å and are typical of anionic polyphosphorus compounds.[13−15]

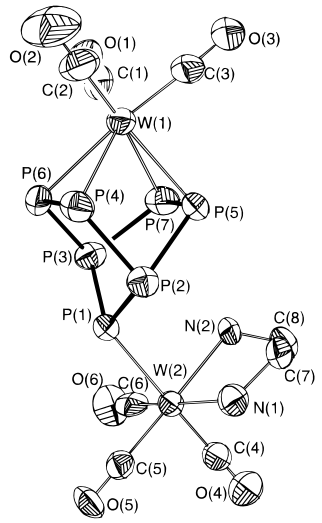

Figure 1. ORTEP drawing of the [(en)$(CO)_3W(\eta^1,\eta^4$-$P_7)W(CO)_3]^{3-}$ ion.

The W(2)−P(1) bond distance of 2.643(3) Å is virtually identical to the average of the W(1)−P contacts but longer than the average W−P single-bond distance in tungsten(0)−phosphine complexes (2.50 Å, average).[16] The W(2)−C bonds *trans* to the W−N bonds are longer than W(2)−C(4), again, consistent with expectations based on the *trans* influence. The W(1)−P(1)−W(2) angle of 135.9(2)° indicates distortion toward planarity at P(1) presumably due to steric pressure of the large $W(CO)_3$(en) fragment.

Crystals of the [K(2,2,2-crypt)]$^+$ salt of **4** are triclinic, space group $P\bar{1}$, and are plagued by a disorder in the $P_7W(CO)_3$ portion of the structure. An ORTEP drawing of the [η^4-$(C_6H_{11})_3SnP_7W(CO)_3]^{2-}$ ion is shown in Figure 2. Although the [K(2,2,2-crypt)]$^+$ and $(C_6H_{11})_3Sn$ portions of the structure were well-behaved and displayed normal metric parameters, the orientational

(10) Ahlrichs, R.; Fenske, D.; Fromm, K.; Krautscheid, H.; Krautscheid, U.; Treutler, O. *Chem. Eur. J.* **1996**, *2*, 238.
(11) Eichhorn, B. W.; Haushalter, R. C.; Pennington, W. T. *J. Am. Chem. Soc.* **1988**, *110*, 8704.
(12) Charles, S.; Eichhorn, B. W.; Bott, S. G.; Fettinger, J. C. *J. Am. Chem. Soc.* **1996**, *118*, 4713.
(13) von Schnering, H. G. In *Rings, Chains, and Macromolecules of Main Group Elements*; Rheingold, A. L., Ed.; Elsevier: Amsterdam, 1977.
(14) von Schnering, H. G. *Angew. Chem., Int. Ed. Engl.* **1981**, *20*, 33.
(15) von Schnering, H. G.; Hönle, W. *Chem. Rev.* **1988**, *88*, 243.
(16) Elmes, P. S.; Gatehouse, B. M.; West, B. O. *J. Organomet. Chem.* **1974**, *82*, 235.

Table 1. Crystallographic Data for $[K(2,2,2\text{-crypt})]_3[(en)(CO)_3W(\eta^1,\eta^4\text{-}P_7)W(CO)_3]\cdot 2en$ and $[K(2,2,2\text{-crypt})]_2[\eta^4\text{-}(C_6H_{11})_3SnP_7W(CO)_3]$

empirical formula	$C_{66}H_{132}K_3N_{12}O_{24}P_7W_2$	$C_{57}H_{105}K_2N_4O_{15}P_7SnW$
fw	2179.63	1683.98
temp, K	293(2)	153(2) K
radiation	Mo Kα ($\lambda = 0.710\ 73$ Å)	Mo Kα ($\lambda = 0.710\ 73$ Å)
crystal system	triclinic	triclinic
space group	$P\bar{1}$	$P\bar{1}$
cell dimens		
a, Å	14.396(4)	12.247(2)
b, Å	17.543(3)	15.1909(14)
c, Å	20.518(2)	21.292(3)
α deg	82.419(11)	97.374(10)
β deg	76.830(14)	93.273(13)
γ deg	69.16(2)	111.217(9)
V, Å^3	4708(2)	3639.2(8)
Z	2	2
d (calcd), g/cm^3	1.538	1.537
abs coeff, mm^{-1}	0.343	2.251
crystal size, mm	0.35 × 0.25 × 0.20	0.500 × 0.275 × 0.100
θ range, deg	2.01−22.48	2.72−22.50
index ranges	$0 \le h \le 15$	$-14 \le h \le 14$
	$-17 \le k \le 18$	$-18 \le k \le 17$
	$-21 \le l \le 22$	$0 \le l \le 25$
no. of reflns collected	12 852	9811
no. of indep reflns	12 261 [R(int) = 0.0577]	9502 [R(int) = 0.0382]
data/restraints/params	12261/0/1017	9502/565/866
goodness-of-fit on F^2	1.027	1.140
final R indices [$F > 4\sigma(F)$]	$R(F) = 0.0552$[a]	$R(F) = 0.1050$[a]
	$R_w(F^2) = 0.1431$[b] [7741 data]	$R_w(F^2) = 0.2021$[b] [6377 data]
largest diff peak and hole, e Å^{-3}	1.246 and −0.816	1.485 and −1.363

[a] $R(F) = \sum|F_o - F_c|/\sum F_o$. [b] $R_w(F^2) = (\sum w|(F_o)^2 - (F_c)^2|^2/\sum wF_o^2)^{1/2}$.

Table 2. Selected Bond Distances (Å) and Angles (deg) for the $[(en)(CO)_3W(\eta^1,\eta^4\text{-}P_7)W(CO)_3]^{3-}$ Ion

		Bonds	
P(1)−P(2)	2.144(4)	P(1)−P(3)	2.149(4)
P(2)−P(4)	2.217(4)	P(2)−P(5)	2.232(5)
P(3)−P(6)	2.214(5)	P(3)−P(7)	2.219(5)
P(4)−P(5)	2.873(5)	P(6)−P(7)	3.192(5)
P(4)−P(6)	2.136(5)	P(5)−P(7)	2.135(5)
P(1)−W(2)	2.643(3)	P(4)−W(1)	2.601(3)
P(5)−W(1)	2.591(3)	P(6)−W(1)	2.670(3)
P(7)−W(1)	2.675(3)	W(1)−C(1)	1.91(2)
W(1)−C(2)	1.91(2)	W(1)−C(3)	1.917(14)
W(2)−C(4)	1.892(14)	W(2)−C(5)	1.950(13)
W(2)−C(6)	1.94(2)	C(1)−O(1)	1.18(2)
C(2)−O(2)	1.19(2)	C(3)−O(3)	1.17(2)
C(4)−O(4)	1.216(14)	C(5)−O(5)	1.153(13)
C(6)−O(6)	1.17(2)	W(2)−N(1)	2.321(9)
W(2)−N(2)	2.327(9)	N(1)−C(7)	1.50(2)
N(2)−C(8)	1.44(2)	C(7)−C(8)	1.55(2)
		Angles	
P(1)−P(2)−P(4)	104.0(2)	P(1)−P(3)−P(7)	107.3(2)
P(2)−P(1)−P(3)	115.0(2)	P(2)−P(4)−P(6)	104.3(2)
P(3)−P(7)−P(5)	103.3(2)	P(4)−P(2)−P(5)	80.5(2)
P(6)−P(3)−P(7)	92.2(2)	P(4)−W(1)−P(5)	67.19(11)
P(4)−W(1)−P(6)	47.79(11)	P(6)−W(1)−P(7)	73.37(11)
P(2)−P(4)−W(1)	105.0(2)	P(3)−P(7)−W(1)	97.0(2)
P(4)−P(6)−W(1)	64.43(12)	P(7)−P(5)−W(1)	68.17(13)
P(4)−W(1)−C(1)	137.7(4)	P(5)−W(1)−C(1)	134.2(4)
P(6)−W(1)−C(3)	174.4(4)	P(7)−W(1)−C(2)	172.7(4)
W(1)−C(1)−O(1)	176.5(13)	W(1)−C(2)−O(2)	179.5(14)
W(1)−C(3)−O(3)	174.7(13)	P(1)−W(2)−C(4)	177.1(4)
P(1)−W(2)−N(1)	86.3(2)	W(2)−C(4)−O(4)	178.6(11)
W(2)−C(5)−O(5)	178.0(10)	W(2)−C(6)−O(6)	178.3(11)
W(2)−N(1)−C(7)	112.4(8)	C(4)−W(2)−C(5)	88.9(5)
C(5)−W(2)−C(6)	83.9(5)	N(1)−W(2)−C(4)	91.0(4)
N(1)−W(2)−N(2)	74.9(4)	N(1)−C(7)−C(8)	109.6(11)

disorder in the $P_7W(CO)_3$ fragment led to high final residuals and a few unreasonable distances and angles in that portion of the ion. For this reason, the metric parameters have been omitted from the present discussion and only the general features of the structure will be described.

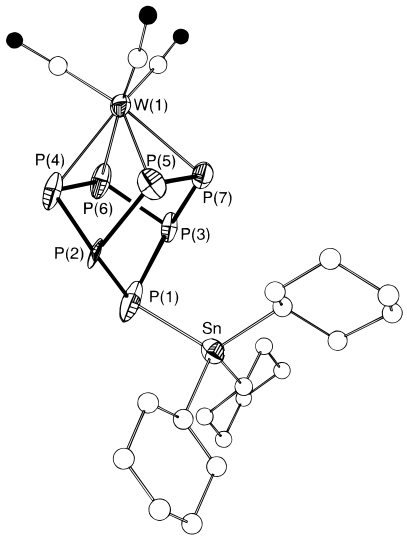

Figure 2. ORTEP drawing of the $[\eta^4\text{-}(C_6H_{11})_3SnP_7W(CO)_3]^{2-}$ ion.

The $[\eta^4\text{-}(C_6H_{11})_3SnP_7W(CO)_3]^{2-}$ ion has the familiar norbornadiene-like η^4-P_7 core with a $(C_6H_{11})_3Sn^+$ group attached to the P(1) atom. The structure is quite similar to that of $[\eta^4\text{-}(C_2H_5)P_7W(CO)_3]^{2-}$, as expected. Despite the disorder, it is clear that the geometry at P(1) is distinctly pyramidal with W−P(1)−Sn angles of 118.2(5) and 124.4(5)° for the two crystallographically observed orientations. These angles are significantly less that those of **3b** described above and only slightly larger than the 116.0(2)° W−P(1)−C angle in $[(C_2H_5)P_7W(CO)_3]^{2-}$.

Spectroscopic Studies. The carbonyl region of the $^{13}C\{^1H\}$ NMR spectra of compounds **3a** and **3b** shows two carbonyl resonances between 236 to 226 ppm due to the two types of $M(CO)_3$ fragments. The $(\eta^4\text{-}P_7)M(\boldsymbol{C}O)_3$ carbons appear downfield of the $(en)(\boldsymbol{C}O)_3W(\eta^1\text{-}P_7)$ carbons. The peak assignments were based on $^{183}W-^{13}C$ couplings observed for the $[(en)(\boldsymbol{C}O)_3W(\eta^1,\eta^4\text{-}P_7)Cr(CO)_3]^{3-}$ resonance ($^1J_{C-W} = 171$ Hz)

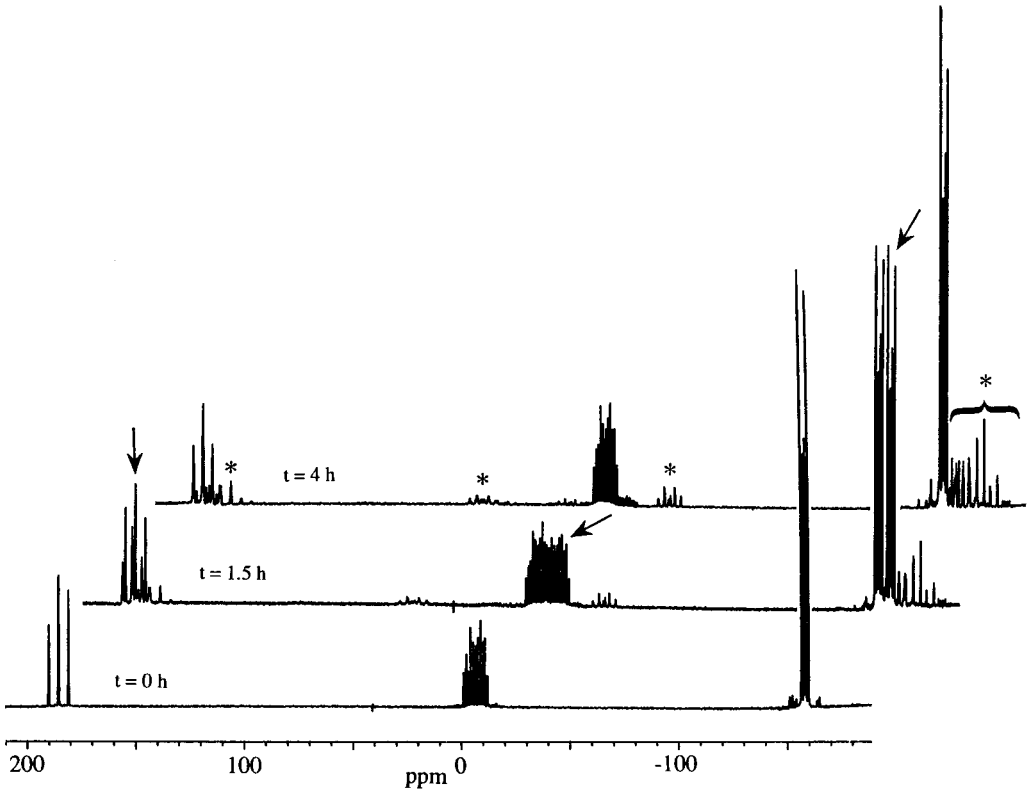

Figure 3. $^{31}P\{^1H\}$ NMR spectra of a crude reaction mixture of $[\eta^4\text{-}P_7W(CO)_3]^{3-}$ and (mesitylene)$W(CO)_3$ giving $[(en)(CO)_3W(\eta^1,\eta^4\text{-}P_7)W(CO)_3]^{3-}$ in DMF-d_7 recorded at $t = 0$ h, $t = 1.5$ h, and $t = 3$ h (bottom to top, respectively) at 27 °C and 81.0 MHz. The asterisks denote impurities. Arrows in the $t = 1.5$ h spectrum denote resonances arising from $[\eta^4\text{-}P_7W(CO)_3]^{3-}$. The horizontal chemical shift axis corresponds to the $t = 0$ spectrum only; the $t = 1.5$ h and $t = 3$ h spectra are offset to the right.

and comparisons with spectra for **3b**. The single resonances for the $\eta^4\text{-}P_7M(\boldsymbol{C}O)_3$ carbons indicate that the $M(CO)_3$ fragments rotate rapidly in the P_4 face of the P_7^{3-} cluster on the NMR time scale, as is common for compounds of this type.[2,4,17] The single (en)$(\boldsymbol{C}O)_3W(\eta^1\text{-}P_7)$ carbonyl resonance of **3a** at 231 ppm shows broadening due to $^{13}C-^{31}P$ coupling ($^2J_{C-P} \approx 2$ Hz), indicating that P_7--$W(en)(CO)_3$ dissociation is *not* occurring on the NMR time scale. Rather, an arm-off/arm-on fluxional process involving the coordinated en ligand is more likely operative that could scramble the CO ligands through a 5-coordinate, 16-electron intermediate. The carbonyl resonances of **3b** are similar to those observed for **3a** with the exception that the downfield carbonyl resonance assigned to the $(\eta^4\text{-}P_7)W(\boldsymbol{C}O)_3$ fragment shows $^{13}C-^{31}P$ coupling ($^2J_{C-P} = 2.5$ Hz) reminiscent of the carbonyl resonance of the parent compound **1b**. There is a downfield shift of the carbonyl resonances of **3** relative to the $M(CO)_6$ compounds (M = Cr, $\delta = 212$ ppm; M = W, $\delta = 192$ ppm)[18] and a small upfield shift relative to the parent compounds **1a** and **1b** (**1a**, $\delta = 246$ ppm; **1b**, $\delta = 232$ ppm).[2] The ^{13}C NMR $W(\boldsymbol{C}O)_3$ chemical shifts for **4** appear at 228 ppm.

The time-lapse $^{31}P\{^1H\}$ NMR spectra showing the formation of the $[(en)(CO)_3W(\eta^1,\eta^4\text{-}P_7)W(CO)_3]^{3-}$ ion **3b** from the reaction of **1b** with (mesitylene)$W(CO)_3$ are given in Figure 3. The three resonances for **3b** are in a 4:2:1 integral ratio, corresponding to the four metal-bound atoms P(4), P(5), P(6), and P(7), the two bridging atoms P(2) and P(3), and the unique phosphorus atom P(1), respectively. The spectra are remarkably similar to those of **1** (see Figure 3) in that the four metal-bound atoms are chemically equivalent on the NMR time scale.[2] Based on the crystal structure of **3b**, one would anticipate seven ^{31}P resonances due to the seven inequivalent phosphorus atoms observed in the solid state (*i.e.*, no crystallographic symmetry). However, the spectra represent AA′A″A‴MM′X spin systems resulting from two independent fluxional processes that are rapid on the NMR time scale at −60 °C and 202 MHz. First, the asymmetries in the P(4)--P(5)/P(6)--P(7) separations observed in the solid state are time-averaged in solution due to an intramolecular wagging process (Scheme 1, path A) that is operative for all compounds **1** and **2**.[2,4] This process generates a virtual mirror plane that bisects the P(4)−P(6) and P(5)−

Scheme 1

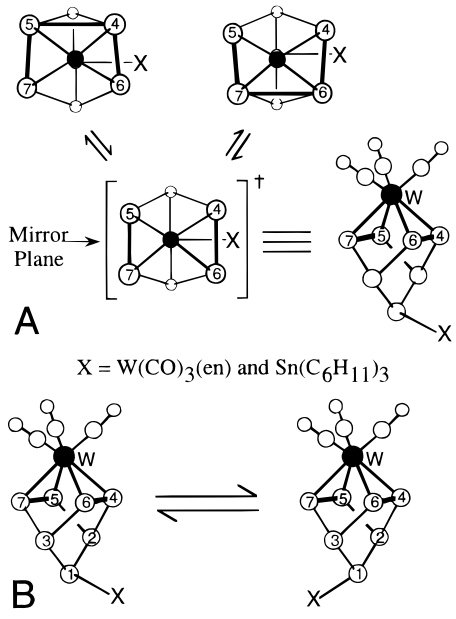

(17) Charles, S.; Eichhorn, B. W.; Fettinger, J. C. In preparation.
(18) Braterman, P. S.; Milne, D. W.; Randall, E. W.; Rosenberg, E. *J. Chem. Soc., Dalton Trans.* **1973**, 1027.

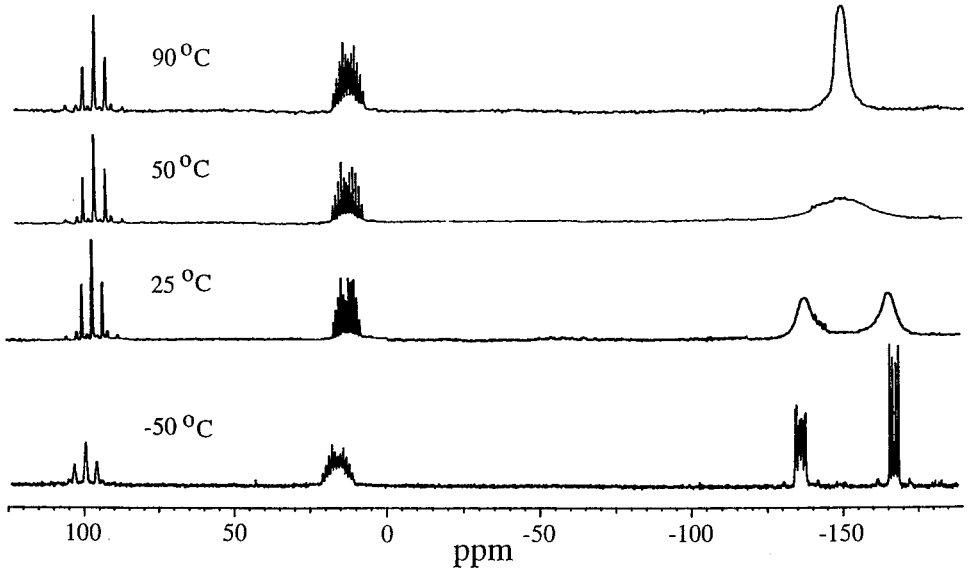

Figure 4. Stacked plot of the $^{31}P\{^1H\}$ NMR spectra for $[\eta^4\text{-}(C_6H_{11})_3SnP_7W(CO)_3]^{2-}$ recorded at various temperatures (see Figure) at 81.0 MHz in DMF-d_7. The upfield resonances that coalesce at high temperatures are due to the tungsten-bound phosphorus atoms. Note that P−Sn coupling for the P(1) resonance is observed at all temperatures.

P(7), bonds making P(4) and P(5) chemically equivalent to P(6) and P(7), respectively. A second process of rapid inversion at P(1) generates an additional virtual mirror plane (Scheme 1, path B), making P(4) and P(6) chemically equivalent to P(5) and P(7), respectively. It is important to note that *both* processes shown in Scheme 1 must be operative in order for all four W(1)-bound phosphorus atoms to become chemically equivalent. The retention of $^{13}C-^{31}P$ coupling between P(1) and the carbonyl ligands of the $W(CO)_3$(en) moiety precludes a dissociative mechanism. Moreover, rapid dissociation of the $W(CO)_3$(en) moiety from **3b** would form **1b** in solution and one would expect time-averaged ^{31}P NMR resonances for mixtures of **3b** and **1b**. It is clear from Figure 3 that **3b** and **1b** coexist in solution and are not exchanging on the NMR time scale.

The variable-temperature ^{31}P NMR spectra for **4** are shown in Figure 4. At −50 °C, two second-order resonances are observed at −138 and −169 ppm, corresponding to the inequivalent pairs of phosphorus atoms bound to the $W(CO)_3$ center, along with the P(2)/P(3) multiplet at 13 ppm and the P(1) pseudotriplet at 98 ppm. The spectrum is quite similar to those of **2**, in which the intramolecular wagging process is rapid on the NMR time scale but inversion at phosphorus is not observed. As the temperature is increased, the two upfield resonances broaden and coalesce at 40 °C (81.0 MHz) while the other two resonances remain sharp. At 90 °C, phosphorus−tin coupling remains constant ($^1J_{Sn-P}$ = 948 Hz) while the inequivalent pairs of $W(CO)_3$-bound phosphorus atoms are approaching the fast-exchange limit. These observations are indicative of a nondissociative inversion of configuration at P(1). From these data, the $\Delta G^{\ddagger}$ for this process was calculated[19] to be 13 kcal/mol.

The IR spectra of **3** show four ν(C−O) vibrations between 1869 and 1734 cm^{-1} which are blue-shifted by ∼35 cm^{-1} from those of the parent compounds **1**. The frequency change is somewhat less than the ∼40 cm^{-1} blue shift for compounds **2**.[4] For comparison, the IR spectrum of **4** shows three bands at 1869, 1774, and 1753 cm^{-1}.

(19) Sandström, J. *Dynamic NMR Spectroscopy*; Academic Press: New York, 1982; p 78.

Scheme 2

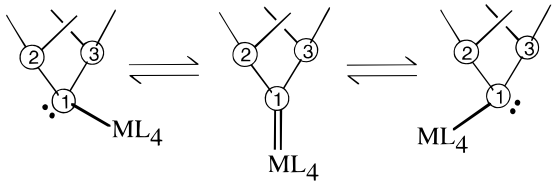

Discussion

The ^1H and ^{13}C NMR data for the $[(en)(CO)_3W(\eta^1,\eta^4\text{-}P_7)W(CO)_3]^{3-}$ ions in DMF-d_7 show resonances consistent with free ethylenediamine, suggesting that the en ligand is dissociating from W(2). A complete dissociation of en or an arm-off/arm-on fluxional process would generate a 5-coordinate, 16-electron metal center at W(2). The formation of an unsaturated intermediate is consistent with the observed intramolecular CO scrambling at W(2) and the displacement of the $W(CO)_3$(en) fragment by a second 1 equiv of P_7^{3-} (see eq 3). Electronic unsaturation at W(2) may also lower the inversion barrier at P(1). It is possible that the second lone pair on P(1) could interact with the 16-electron W(2) center in a π fashion to generate partial double-bond character that could stabilize a planar transition state (see Scheme 2). This mechanism is clearly operative in phosphido compounds[20−22] and has also been proposed for other cases of pyramidal inversion at other main group elements bound to transition metals [*i.e.*, *cis*-bis(dibenzyl sulfide)dichloroplatinum(II) (E_a = 18.0 kcal/mol)].[23] However, π-bonding is presumably not involved in lowering the inversion barrier in **4** and is unlikely to be significant in **3** if the M−P contacts in the 16-electron transition state are similar to those observed in the crystal structure.

Numerous papers and reviews have been presented on such mechanisms involving inversion at nitrogen, phosphorus, and sulfur.[24,25] Typical ranges for barriers of inversion (E_a) are 4−8 kcal/mol for trialkylamines, 29−40 kcal/mol for trialkylphos-

(20) Buhro, W. E.; Gladysz, J. A. *Inorg. Chem.* **1985**, *24*, 3505.
(21) Buhro, W. E.; Zwick, B. D.; Georgiou, S.; Hutchinson, J. P.; Gladysz, J. A. *J. Am. Chem. Soc.* **1988**, *110*, 2427.
(22) Buhro, W. E.; Chisholm, M. H.; Folting, K.; Huffman, J. C.; Matrin, J. D.; Streib, W. E. *J. Am. Chem. Soc.* **1992**, *114*, 557.
(23) Haake, P.; Turley, P. C. *J. Am. Chem. Soc.* **1967**, *89*, 4617.
(24) Lambert, J. B. *Top. Stereochem.* **1971**, *6*, 19.

phines, 25−29 kcal/mol for sulfonium ions, and 35−42 kcal/mol for sulfoxides.[24,25] Bulky electropositive substituents lower the barriers to inversion as illustrated by the silylphosphines where E_a is lowered to *ca.* 19 kcal/mol. In many cases, the origins for low barriers to inversion at phosphorus in specific compounds are attributed to various sources that include steric effects, substituent electronegativities, and conjugation with a transition metal.[26,27]

The first observation of inversion at phosphorus in a polycyclophosphane was reported by Baudler *et al.* for the compounds P_9R_3 (R = Et, *t*-Bu). The inversion barrier (E_a) for P_9-*t*-Bu_3 was determined to be 18.5 kcal/mol, which is in the range of inversion barriers for open-chain organophosphanes with P−P bonds in their molecular skeletons.[8,25,26,28] It is reported that inversion was slower in P_9Et_3 than in P_9-*t*-Bu_3, but an activation barrier was not reported. Inversion is also observed for other polycyclophosphanes, including P_{11}-*i*-Pr_3, P_{12}-*i*-Pr_4, P_{13}-*i*-Pr_5, and P_{14}-*i*-Pr_4.[8,9,28] Barriers to inversion for these compounds were found to be qualitatively higher than that for P_9-*t*-Bu_3.

The origin of the low inversion barriers at P(1) in compounds **3** and **4** may be due to a combination of effects, such as the π-bonding effects just described, steric effects, or the effective electronegativity of the attached substituent. However, it is difficult to separate the individual contributions of each effect. For an assessment of the steric crowding at P(1), we monitored the W(1)−P(1)−X angles in the $[\eta^4$-$XP_7W(CO)_3]^{3-}$ compounds (see drawing of **2**). A planar P(1) geometry would give a 180° angle whereas the apparently uncrowded P(1) atom in $[(\eta^4$-$EtP_7)W(CO)_3]^{2-}$ has a 116.0° W(1)−P(1)−C angle. The P(1) atom in $[(en)(CO)_3W(\eta^1,\eta^4$-$P_7)W(CO)_3]^{3-}$ is distinctly less pyramidal than that in the other two crystallographically characterized examples with a W(1)−P(1)−W(2) angle of 135.9°. However, this steric destabilization due to the large $W(CO)_3$(en) group on P(1) is probably not the only factor in lowering the inversion at P(1) in that $[(\eta^4$-$(C_6H_{11})_3SnP_7)W(CO)_3]^{2-}$ shows little sign of steric strain (W(1)−P(1)−Sn = 121.3°, average) yet it too has a low barrier to inversion. A systematic investigation of the $[\eta^4$-$XP_7W(CO)_3]^{3-}$ compounds is in progress in an attempt to separate the electronic effects from the steric effects.

Experimental Section

General Data. General operating procedures used in our laboratory were described previously.[2] All IR spectra were recorded from KBr pellets on a Nicolet Model 5DXC FT IR spectrophotometer under an N_2 purge. Carbon (^{13}C) NMR spectra were recorded at ambient temperature on Bruker AF200 (50.324 MHz) and Bruker AM400 (100.614 MHz) spectrometers. Some of the ^{13}C NMR chemical shifts and couplings were confirmed by recording the spectra at different magnetic field strengths. Phosphorus (^{31}P) NMR spectra were recorded on a Bruker WP200 (81.015 MHz) spectrometer. By convention, $+\delta$ chemical shifts are downfield of zero. Elemental analyses were performed under inert atmospheres by Desert Analytics, Tucson, AZ.

Chemicals. The preparation of the K_3P_7 was previously reported.[2] (Mesitylene)chromium tricarbonyl, (mesitylene)tungsten tricarbonyl, and 2,2,2-crypt were purchased from Aldrich and used without further purification. The $[\eta^4$-$P_7M(CO)_3]^{3-}$ ions (M = Cr, W) were prepared according to literature methods.[2] Ethylenediamine was purchased from Fisher (Anhydrous), distilled several times from CaH_2 under N_2 and then from K_4Sn_9 at reduced pressure, and finally stored under N_2. DMF was purchased from Burdick & Jackson (High Purity), degassed, distilled at reduced pressure from K_4Sn_9, and stored under N_2. DMF-d_7 was purchased from Cambridge Isotope Laboratories and degassed.

Syntheses. Preparation of $[K(2,2,2\text{-crypt})]_3[(en)(CO)3W(\eta^1,\eta^4$-$P_7)Cr(CO)_3]\cdot 2en$. K_3P_7 (29.6 mg, 0.089 mmol), 2,2,2-crypt (100.0 mg, 0.27 mmol), and (mesitylene)$Cr(CO)_3$ (22.7 mg, 0.089 mmol) were combined in en (∼3 mL), and the mixture was stirred for 12 h, producing an orange solution. (Mesitylene)$W(CO)_3$ (34.4 mg, 0.089 mmol) was added as a solid, and the reaction mixture was stirred for an additional 4 h, yielding a dark red solution with a dark red powder precipitate. The solution was warmed gently (∼35 °C) to redissolve the precipitate and then allowed to slowly cool to ambient temperature. After 24 h, the reaction vessel contained a dark red microcrystalline solid. The solid was removed from the mother liquor, washed with toluene, and dried under vacuum (microcrystalline yield 76 mg, 53%). IR (KBr pellet), ν(C−O) cm^{-1}: 1869 (m), 1848 (s), 1760 (sh), 1734 (s). $^{13}C\{^1H\}$ NMR (DMF-d_7) δ (ppm): 236 [s, Cr(*C*O)$_3$], 231 [m, $^1J_{C-W}$ = 171 Hz, W(*C*O)$_3$]. $^{31}P\{^1H\}$ NMR (DMF-d_7) δ (ppm): 187 [t, $^1J_{P-P}$ = 364 Hz, 1 P, P(1)], −5 [second-order multiplet, 2 P, P(2, 3)], −157 [second-order multiplet, 4 P, P(4, 6) and P(5, 7)]. Anal. Calcd for $C_{66}H_{132}K_3N_{12}O_{24}P_7CrW$: C, 38.71; H, 6.50; N, 8.21. Found: C, 38.4; H, 6.34; N, 6.75. The low nitrogen content is indicative of en solvate loss during transport and analysis.

Preparation of $[K(2,2,2\text{-crypt})]_3[(en)(CO)_3W(\eta^1,\eta^4$-$P_7)W(CO)_3]\cdot 2en$. A procedure identical to that described for $[K(2,2,2\text{-crypt})]_3[(en)(CO)_3W(\eta^1,\eta^4$-$P_7)Cr(CO)_3]\cdot$2en was followed except (mesitylene)$W(CO)_3$ (34.4 mg, 0.089 mmol) was used in the reaction instead of (mesitylene)$Cr(CO)_3$. After 24 h, the reaction vessel contained a dark red microcrystalline solid. The solid was removed from the mother liquor, washed with toluene, and dried under vacuum (microcrystalline yield 116 mg, 60%). IR (KBr pellet), ν(C−O) cm^{-1}: 1869 (m), 1849 (s), 1759 (sh), 1736 (s). $^{13}C\{^1H\}$ NMR (DMF-d_7) δ (ppm): 230 [m, $^2J_{C-P}$ = 2.5 Hz, W(*C*O)$_3$], 226 [m, W(en)(*C*O)$_3$]. $^{31}P\{^1H\}$ NMR (DMF-d_7) δ (ppm): 187 [tm, $^1J_{P-P}$ = 353 Hz, $^2J_{P-P}$ = 16 Hz, 1 P, P(1)], 2 [second-order multiplet, 2 P, P(2, 3)], −153 [second-order multiplet, 4 P, P(4, 6) and P(5, 7)]. Anal. Calcd for $C_{66}H_{132}K_3N_{12}O_{24}P_7W_2$: C, 36.37; H, 6.10; N, 7.71. Found: C, 36.29; H, 5.95; N, 7.96.

Exchange Reaction. $[K(2,2,2\text{-crypt})]_3[(en)(CO)_3W(\eta^1,\eta^4$-$P_7)Cr(CO)_3]\cdot$2en was prepared in en as described above but not isolated. K_3P_7 (29.6 mg, 0.089 mmol) was added *in situ* as a solid and the reaction mixture stirred for an additional 12 h. An aliquot was removed and analyzed by ^{31}P NMR spectroscopy.

Preparation of $[K(2,2,2\text{-crypt})]_2[\eta^4$-$(C_6H_{11})_3SnP_7W(CO)_3]$. $[\eta^4$-$P_7W(CO)_3]^{3-}$ (0.089 mmol) was prepared *in situ* as a red powder suspended in en (3 mL) as described above. One equivalent (based on P_7^{3-}) of $(C_6H_{11})_3SnCl$ (34.2 mg, 0.089 mmol) was added to the reaction mixture, and the solution was stirred overnight. A reddish-brown solution containing a brown powdery precipitate resulted. The reaction mixture was heated gently (∼40 °C), the precipitate dissolved, and the solution became clear, dark red. The solution was then filtered through 0.5 in. of tightly packed glass wool in a pipet. Subsequent gradual cooling to room temperature yielded dark reddish-brown crystals after 12 h. The crystals were removed from the mother liquor, washed with toluene, and then dried *in vacuo* (crystalline yield 63 mg, 42%). IR (KBr pellet), ν(C−O) cm^{-1}: 1869 (vs), 1774 (s), 1753 (s). ^{31}P NMR (DMF-d_7, −50 °C) δ (ppm): 98 (1 P, triplet with $^{117/119}Sn$ satellites, $^1J_{P-P}$ = 307 Hz, $^2J_{P-P} \approx$ 12 Hz, $^1J_{P-Sn} \approx$ 948 Hz), 13 (2 P, second-order multiplet), −138 (2 P, second-order multiplet), −169 (2 P, second-order multiplet). ^{13}C NMR (DMF-d_7, 25 °C) δ (ppm): 228 ($^1J_{C-W}$ = 176 Hz), 33.13, 30.08, 30.04 (obscured by the solvent septet), 27.62. ^1H NMR (DMF-d_7, 25 °C) δ (ppm): 1.99, 1.59, 1.26 (multiplets). Anal. Calcd for $C_{57}H_{105}K_2N_4O_{15}P_7SnW$: C, 40.65; H, 6.28; N, 3.33. Found: C, 40.43; H, 6.03; N, 3.94.

X-ray Crystallographic Studies. $[K(2,2,2\text{-crypt})]_3$3b·2en. An orange-red crystal of dimensions 0.35 × 0.25 × 0.20 mm with a parallelepiped habit was placed on an Enraf-Nonius CAD-4 diffractometer. The crystal's final cell parameters and crystal orientation matrix were determined from 25 reflections in the range $20.0° < 2\theta < 30.5°$; these constants were confirmed with axial photographs. Data were collected [Mo Kα] with $\omega-2\theta$ scans over the range 2.0−22.5° using a variable scan speed of 3.3−16.48° min^{-1}, with each scan being

(25) Rauk, A.; Allen, L. C.; Mislow, K. *Angew. Chem., Int. Ed. Engl.* **1970**, *9*, 400.
(26) Baechler, R. D.; Mislow, K. *J. Am. Chem. Soc.* **1971**, *93*, 773.
(27) Ranaivonjatovo, H.; Escudie, C.; Couret, C.; Declercq, J.-P.; Dubourg, A.; Satge, J. *Organometallics* **1993**, *12*, 1674.
(28) Baudler, M.; Hahn, J.; Koll, B.; Kazmierczak, K.; Darr, E. *Z. Anorg. Allg. Chem.* **1986**, *538*, 7.

recorded in 96 steps with the outermost 16 steps on each end of the scan being used for background determination. Minor, 1−3%, variations in intensity were observed; data were not corrected. Three ψ-scan reflections were collected over the range 7.2−11.6°, with transmission factors ranging from 0.7764 to 0.9971; average 0.8974. Data were corrected for Lorentz and polarization factors and for absorption and were reduced to observed structure factor amplitudes. Intensity statistics clearly favored the triclinic centrosymmetric space group $P\bar{1}$ (No. 2). Data were exported as F_o^2 and ($\sigma(F_o^2)$) to the crystallographic program package SHELX.[29] The structure was determined with the successful location of both tungsten atoms. Subsequent difference-Fourier maps revealed the location of the remaining non-hydrogen atoms. The structure was refined to convergence with $R(F) = 11.06\%$, $R_w(F^2) = 15.76\%$, and GOF = 1.027 for all 12261 unique reflections [$R(F) = 5.52\%$ and $R_w(F^2) = 14.31\%$ for those 7741 data with $F_o > 4(F_o)$]. A final difference-Fourier map possessed several peaks within ∼1.2 Å of tungsten atoms with $|\Delta\rho| \leq 1.25$ e Å^{-3}.

[K(2,2,2-crypt)]$_2$4. A reddish orange crystal of dimensions 0.500 × 0.275 × 0.100 mm was placed on the Enraf-Nonius CAD-4 diffractometer. The crystal's final cell parameters and crystal orientation matrix were determined from 25 reflections in the range $17.5 < \theta < 19.0°$; these constants were confirmed with axial photographs. Data were collected as described above. A linear decrease of approximately 20% in intensity for all three standards was observed; data were corrected. Seven ψ-scan reflections were collected over the range $5.9 < \theta < 13.8°$; the absorption correction was applied with transmission factors ranging from 0.5300 to 0.9355.

Data were processed as described above. The structure was determined by direct methods (SHELXS) with the successful location of the tungsten, tin, several phosphorus atoms, and the two potassium atoms. Several subsequent difference-Fourier maps revealed the location of the atoms comprising the cyclohexyl groups along with the two cryptand molecules. Since both cryptand molecules possess chains that are chemically identical, those considered best were used as templates for the others using SAME instructions throughout the refinement process. The two cryptand molecules and the $Sn(C_6H_{11})_3$ groups refined well. It was apparent that the disorder within the complex was within the $WP_7(CO)_3$ group itself, and this was eventually determined to be composed of two units, major:minor 0.55042:0.44958, rotated away from each other with the P(1) atom acting as a point for this rotation. Three carbonyl ligands were now located for each of the two fragments, with one of these carbonyl ligands fully occupied and present in both fragments. The carbon atom of this carbonyl may be considered to be a composite atom. Hydrogen atoms were placed in calculated positions. EXYZ, EADP, SAME, SIMU, and ISOR instructions were invoked where necessary. The structure was refined to convergence [$\Delta/\sigma \leq 0.001$] with nearly all non-hydrogen atoms anisotropic (C(2) refined isotropically), with $R(F) = 15.33\%$, $R_w(F^2) = 22.69\%$, and GOF = 1.140 for all 9502 unique reflections [$R(F) = 10.50\%$ and $R_w(F^2) = 20.21\%$ for those 6377 data with $F_o > 4\sigma(F_o)$]. A final difference-Fourier map possessed a set of highest peaks in the vicinity of either W(1) or W(1A) with $|\Delta\rho| \leq 1.49$ e Å^{-3}; the largest other spurious peaks had $|\Delta\rho| \leq 0.99$ e Å^{-3}. Although the crystal structure clearly shows the general structure of the anion and confirms the pyramidal nature at P(1), the disorder in the $WP_7(CO)_3$ fragment and correspondingly high residuals preclude any meaningful analysis of the bond distances and angles.

Acknowledgment. This work was funded by the National Science Foundation through Grant CHE-9500686.

Supporting Information Available: A description of the structure determinations for [K(2,2,2-crypt)]$_3$[(en)(CO)$_3$W(η^1,η^4-P$_7$)W(CO)$_3$]·2en and [K(2,2,2-crypt)]$_2$[η^4-(C_6H_{11})$_3$SnP$_7$W(CO)$_3$] (2 pages). X-ray crystallographic files, in CIF format, for the two structures are available on the Internet only. Ordering and access information is given on any current masthead page.

IC961177Q

(29) Sheldrick, G. *Acta. Crystallogr.* **1990**, *A46*, 467.